J.Mycopathol.Res. 63(1) : 109-119, 2024, ISSN : 0971-3719 (Print), 2583-6315 (Online) 10.57023/JMycR.63.1.2025.109

Castor oil nanoemulsion inhibits *Streptococcus mutans* and *Candida albicans* biofilms in periodontitis

ATRAYEE DAS GUPTA*, JAYITA GHOSH, SHUBHAM KUMAR, ARNAB GANGULI AND SUKANTA BHADRA

Department of Microbiology, Techno India University, West Bengal EM-4 Sector-V, Saltlake City, Kolkata- 700091, West Bengal

Received : 25.08.2024 Accepted : 12.02.2025 Published : 31.03.2025

This study investigates the potential of castor oil nanoemulsions (CONEs) in inhibiting biofilms of *Streptococcus mutans* and *Candida albicans*, key pathogens in periodontitis. The nanoemulsion was characterized by dynamic light scattering (DLS), revealing an average droplet size of 75.3 nm, a polydispersity index (PDI) of 0.671, and a zeta potential of -24.69 mV, indicating moderate stability. The minimum inhibitory concentration (MIC) assay showed that CONEs effectively inhibited *S. mutans* at 50 µg/ml, *C. albicans* at 75 µg/ml, and their mixed culture at 100 µg/ml. Further, CONEs demonstrated significant antibiofilm activity, reducing biofilm biomass by 73% for *S. mutans*, 61% for *C. albicans*, and 48% for the mixed culture. The disc diffusion assay confirmed this antimicrobial efficacy, showing inhibition zones of 22 mm for *S. mutans*, 19 mm for *C. albicans*, and 11 mm for the mixed culture. The study also found that CONEs significantly reduced the number of sessile cells and extracellular polymeric substances (EPS) production, key components of biofilm integrity. Additionally, an in silico docking study suggested that ricinoleic acid, a component of CONEs, strongly binds to biofilm-related proteins, further supporting its potential as a therapeutic agent against periodontitis. These findings highlight CONEs as a promising strategy for managing biofilm-associated infections in periodontitis.

Keywords: Dental caries, dynamic light scattering, microbial cells, ricinoleic acid

INTRODUCTION

Periodontitis is a chronic inflammatory disease that affects the supporting structures of the teeth, including the gingiva, periodontal ligament, and alveolar bone (Ray, 2023). It is a major cause of tooth loss in adults and has been linked to systemic conditions such as cardiovascular disease, diabetes, and respiratory infections (Könönen *et al*. 2019). The pathogenesis of periodontitis is complex and multifactorial, involving a combination of microbial, host, and environmental factors (Martínez-García and Hernández-Lemus, 2021). A key feature of periodontitis is the formation of biofilms on the surfaces of teeth and gums. Biofilms are structured communities of microorganisms encased in a self-produced extracellular matrix, which provides protection from the host immune response and antimicrobial agents (Könönen *et al*. 2019). In the oral cavity, biofilms play a central role in the development and progression of periodontal disease (Singh *et al*. 2017). The subgingival biofilm is particularly important, as it harbors pathogenic bacteria that drive the inflammatory process (Mendhe *et al*. 2023).

Among the numerous microbial species implicated in periodontitis, *Streptococcus mutans* and *Candida albicans* are notable for their ability to form robust biofilms (Bachtiar and Bachtiar, 2018). *S. mutans* is a Gram-positive bacterium commonly associated with dental caries, but it also contributes to the pathogenesis of periodontitis through its acidogenic and aciduric properties, which disrupt the local environment and promote the growth of other pathogenic

*Correspondence : atrayeeroydasgupta10@gmail.com

species (Forssten *et al*. 2010). *C. albicans* is a fungal pathogen that can co-infect with bacteria in multispecies biofilms, enhancing the virulence and resilience of the microbial community (Morales and Hogan, 2010).

Natural products have gained attention as potential alternatives or adjuncts to conventional antimicrobial therapies (Hobson *et al*. 2021). Castor oil, derived from the seeds of *Ricinus communis*, has been used traditionally for its medicinal properties, including antimicrobial, anti-inflammatory, and analgesic effects (Mittal and Jaitak, 2019). The antimicrobial activity of castor oil is attributed to its high content of ricinoleic acid, a fatty acid with potent antimicrobial properties (Van Vuuren and Viljoen, 2011).

Nanoemulsions are fine oil-in-water emulsions with droplet sizes typically in the range of 20-200 nm (Pathania *et al*. 2018). They offer several advantages over conventional emulsions, including improved stability, enhanced bioavailability, and greater surface area for interaction with microbial. Nanoemulsions can effectively deliver lipophilic compounds, such as ricinoleic acid, to the site of infection, potentially enhancing their antimicrobial efficacy(Pathania *et al*. 2018)

The objective of this study is to evaluate the efficacy of castor oil nanoemulsion in inhibiting individual and multispecies biofilms of *Streptococcus mutans* and *Candida albicans*, two organisms responsible for the disease periodontitis (Okonogi *et al*. 2021). By investigating the antimicrobial properties of castor oil nanoemulsion, we aim to explore its potential as a novel therapeutic agent for the management of periodontitis (Haq *et al*. 2023).

MATERIALS AND METHODS

Preparation of Castor Oil Nanoemulsion

Castor oil nanoemulsion was prepared using a combination of Castor oil (Sigma-Aldrich), Double Distilled Water (DDW), Tween 80 (Sigma-Aldrich), and an ultrasonic technique for emulsification (Katzer *et al*. 2014). Initially, Castor oil (10% v/v) and Tween 80 (2% v/v) were mixed thoroughly using a magnetic stirrer at room temperature to form the oil phase. Separately, DDW was heated to approximately 70°C and then slowly added to the oil phase under continuous stirring to form a pre-emulsion mixture (Poorani et al., 2016). The pre-emulsion was then subjected to ultrasonication (Sonics Vibra Cell VCX 130, 20 kHz, 150 W) for 10 mins at an amplitude of 50% to achieve nano-sized droplets (El-Naby et al., 2024). The resulting nanoemulsion was cooled to room temperature and stored in amber glass vials to protect it from light-induced degradation until further use (Poorani *et al*. 2016).

Characterization of Castor Oil Nanoemulsion Using Dynamic Light Scattering (DLS)

The castor oil nanoemulsion prepared as described previously was characterized using Dynamic Light Scattering (DLS) to determine the particle size distribution and zeta potential (Oliveira *et al*. 2017). Measurements were performed using a Zetasizer Nano ZS instrument (Malvern Panalytical) equipped with a 633 nm laser at a scattering angle of 173°. Prior to analysis, the nanoemulsion samples were diluted appropriately with DDW to ensure optimal measurement conditions (Loureiro Contente *et al*. 2020). For particle size analysis, measurements were conducted at 25°C, and each sample was measured in triplicate to ensure reproducibility (El-Naby *et al*. 2024). Zeta potential measurements were performed to assess the surface charge of the nanoemulsion particles, providing insights into their stability and potential interactions with microbial cells. Data analysis was performed using the instrument's software to obtain mean particle size and polydispersity index (PDI) values, as well as zeta potential measurements.

Determination of Minimum Inhibitory Concentration (MIC) of Castor Oil Nanoemulsion (CONEs)

The MIC values of Castor oil nanoemulsion (CONEs) against *Streptococcus mutans* and *Candida albicans* were determined using a broth microdilution assay in a 96-well microtiter plate (Rudrapal, 2023). First, CONEs were serially diluted in sterile Mueller-Hinton Broth (MHB) to

concentrations of 10, 25, 50, 75, and 100 µg/mL. Each well of the microtiter plate was inoculated with 100 µL of standardized bacterial or fungal cell suspension (~10^6 CFU/mL). The microplates were then incubated aerobically at 37°C for 24 hours (Guidotti-Takeuchi et al., 2022). After incubation, the optical density (OD) of each well was measured at 600 nm using a spectrophotometer (Thermo Scientific Multiskan GO). The MIC was defined as the lowest concentration of CONEs at which no visible bacterial or fungal growth was observed, indicated by an OD reading comparable to the negative control (MHB without CONEs) (Guidotti-Takeuchi *et al*. 2022). All experiments were conducted in triplicate to ensure reproducibility and reliability of results.

Disc Diffusion Assay

Following the determination of MIC values using a broth microdilution assay, a disc diffusion assay was performed to assess the antimicrobial activity of Castor oil nanoemulsion (CONEs) against *Streptococcus mutans* and *Candida albicans*. Sterile Mueller-Hinton Agar (MHA) plates were prepared, and bacterial or fungal suspensions (~10^6 CFU/mL) were evenly spread across the surface of the agar using a sterile swab (Espinel-Ingroff *et al*. 1991). Using sterile forceps, paper discs were impregnated with CONEs at concentrations equivalent to MIC and half MIC values, as determined previously. The discs were then placed on the inoculated agar plates and gently pressed down to ensure contact with the agar surface (Kavanagh et al., 2019). Plates were incubated aerobically at 37°C for 24 hours to allow for microbial growth. After incubation, the diameter of the inhibition zones around each disc was measured using a calibrated ruler (Tullio *et al*. 2007). The presence and size of inhibition zones indicated the antimicrobial activity of CONEs against *S. mutans* and *C. albicans*. Each assay was performed in triplicate to ensure reliability and reproducibility of results.

Antibiofilm Assay

The antibiofilm activity of Castor oil nanoemulsion (CONEs) against *Streptococcus mutans* and *Candida albicans* was evaluated using a modified version of previously published procedures (Das *et al*. 2020). Biofilms were developed by inoculating LB medium supplemented with MIC and half MIC concentrations of CONEs in a 24-well microtiter plate. Each well was seeded with standardized bacterial or fungal suspensions and incubated for 48 hours at 37°C to allow biofilm formation.

Following incubation, the planktonic LB medium was carefully removed from each well, and the wells were washed twice with sterile distilled water to remove non-adherent cells. The remaining biofilms were stained with 1% crystal violet solution and incubated for 30 mins at 37°C. After staining, excess crystal violet was removed, and the plates were washed again with sterile distilled water before air-drying for 1 hr at 37°C. To quantify biofilm biomass, the stained biofilms were dissolved in 200 ìL of 95% ethanol, and the optical density (OD) was measured at 595 nm using a spectrophotometer (Thermo Scientific Multiskan GO). The percentage of biomass formation was calculated using the formula:

Percentage of Biofilm Formation = [{Test sample OD595 nm / Control sample OD595 nm} × 100] (Rajamani *et al*. 2019).

To determine the number of sessile cells, adherent bacteria in each well were resuspended by vigorous pipetting and vortexing, followed by 30-second sonication. The resulting suspensions were serially diluted (10^-6 to 10^-8) and plated on Luria Agar (LA) plates. After incubation at 37°C for 24 hours, bacterial colonies were counted to assess the viability and density of biofilm-associated cells (Das *et al*. 2023).

Visualization of Biofilms Assay

To visualize the antibiofilm activity of Castor oil nanoemulsion (CONEs), small glass slides (1 × 1 cm) were placed in the wells of a 12-well polystyrene microtiter plate. LB medium supplemented with MIC and half MIC concentrations of CONEs was inoculated with standardized bacterial and fungal suspensions for individual and mixed culture conditions. The microtiter plate was then incubated at 37°C for 48 hrs to allow biofilm formation on the glass

slides. After incubation, planktonic cells were carefully removed by washing with sterile distilled water, and the biofilms on the glass slides were stained with 1% crystal violet dye for 5 mins. Excess dye was gently rinsed off with deionized water, and the slides were air-dried for 5 mins at room temperature. Biofilms were visualized using a light microscope (Magnus MLXi-TR) equipped with Magvision software at 40× magnification. Photographs of the biofilms were taken using a digital camera attached to the microscope. The images were analyzed to assess the morphology, thickness, and coverage of biofilms treated with CONEs compared to untreated controls.

EPS Production Assay

To evaluate the effect of Castor oil nanoemulsion (CONEs) on extracellular polymeric substance (EPS) production by *Streptococcus mutans* and *Candida albicans*, bacterial cultures were grown in LB medium in 24-well plates at 28 ± 2°C for 24 hrs with and without nanoemulsion treatment at MIC and half MIC concentrations . After incubation, non-adherent cells were carefully aspirated and removed from the wells. Biofilm-associated cells were then collected by aspirating and suspending them in 0.5% NaCl solution. The suspended cells were transferred to new sterile test tubes, and an equal volume of phenol (5%) was added to each tube to stabilize EPS. Subsequently, 5 volumes of concentrated sulfuric acid containing 0.2% hydrazine sulfate were added to the solution, and the mixture was incubated for 1 hr in the dark to develop color. The absorbance of each sample was measured at 490 nm using a spectrophotometer (Thermo Scientific Multiskan GO). The absorbance readings at 490 nm provided quantitative data on the amount of EPS produced by biofilm-associated cells treated with CONEs compared to untreated controls.

In Silico Study

In our study, the Als3 adhesin protein of *Candida albicans* and Sortase A protein of *Streptococcus mutans* were selected as the receptor molecules. The PDB files for these proteins were retrieved from the Protein Data Bank and prepared using the AutoDock Vina program. Ricinoleic acid, the active component of castor oil, was chosen as the ligand. The 2-D structure of ricinoleic acid was downloaded from PubChem and prepared using the AutoDock Vina program. The docking simulations were performed to predict the ligand-binding affinities, which were expressed as negative Gibbs free energy scores. These scores were calculated based on the AutoDock Vina scoring function, indicating the strength and stability of the binding interaction between the ligand and the receptor proteins. Post-docking analyses were conducted using PyMOL and LigPlot+ to visualize the docking results and determine the interaction details. These visualizations included the identification of binding sites, hydrogen-bond interactions, hydrophobic interactions, and bonding distances. The interaction ratios were measured as less than 5 Å from the position of the docked ligand, providing insights into the specific molecular interactions between ricinoleic acid and the receptor proteins. The molecular dynamics simulation study was conducted for the ligand, ricinoleic acid, which was identified as the best ligand among the selected molecules from our docking analysis. The molecular dynamics simulation study of the ricinoleic acid-Als3 adhesin and ricinoleic acid-Sortase A docked complexes was performed using the iMODS server. iMODS is a fast, user-friendly, and effective molecular dynamics simulation tool used to investigate the structural dynamics of protein complexes. iMODS provides detailed insights into several structural dynamics parameters including deformability, B-factor (mobility profiles), eigenvalues, variance, covariance map, and elastic network. In this study, the deformability was assessed by examining the ability of each amino acid residue to deform within the complex. The B-factor profiles were analyzed to understand the mobility of the protein residues. The eigenvalue, which is inversely related to the ease of deformability, was determined to evaluate the energy required to deform the given protein-ligand complex structure. A lower eigenvalue indicates easier deformability and higher flexibility of the complex. Additionally, the eigenvalue represents the motion stiffness of the protein complex.

RESULTS AND DISCUSSION

Characterization of Castor Oil Nanoemulsion (CONEs)

The castor oil nanoemulsion (CONEs) prepared using ultrasonic emulsification was characterized

by dynamic light scattering (DLS) to determine its hydrodynamic size, polydispersity index (PDI), and zeta potential. The DLS analysis revealed that the CONEs had an average droplet size of 75.3 ± 2.7 nm, indicating that the nanoemulsion droplets were in the nanometric range (Fig 1). The high-energy shear forces induced by ultrasonic treatment were primarily responsible for achieving this nano-sized distribution, as they efficiently broke down the oil droplets into smaller sizes (Wallock-Richards *et al.* 2015).

Further analysis showed that the PDI value of CONEs was 0.671, suggesting a moderate degree of uniformity in droplet size distribution.

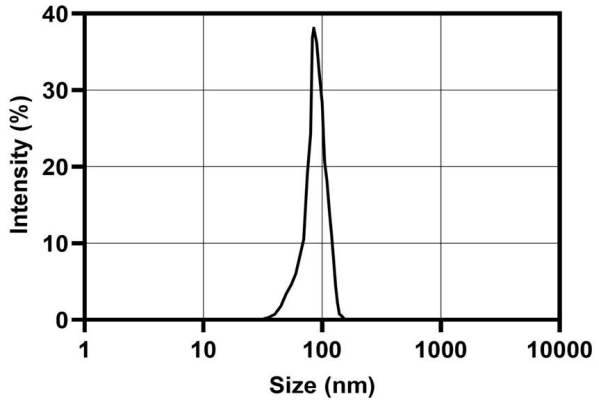

Fig. 1: Particle size (nm) distribution by intensity (%) of castor oil nano-emulsion.

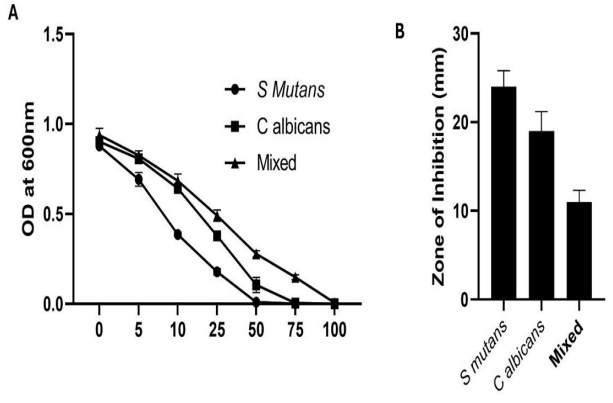

Fig.2: Crystal violet assay indicating significant reduction in biofilm biomass of *Streptococcus mutans, Candida albicans* and the mixed culture upon treatment with CONEs **(Fig.2A**).

The MIC of CONEs resulting reduction of sessile cells for *Streptococcus mutans*, *Candida albicans*, and the mixed culture **(Fig.2A.)**.

Disc diffusion of CONE with *Streptococcus mutans*, *Candida albicans*, and the mixed culture **(Fig. 2B)**

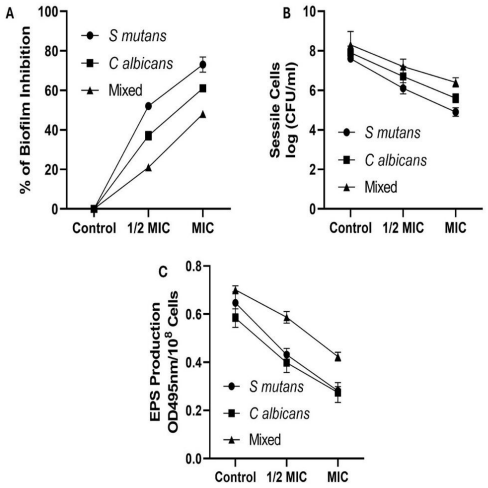

Fig.3: Reduction of EPS production in the biofilms **(Fig. 3C)** increases the inhibition of biofilm formation **(Fig.3A)** and decreases the sessile cell count (CFU/ml) **(Fig.3B)** of *Streptococcus mutans* and *Candida albicans,* and the mixed culture upon treating with MIC of Castor oil nano-emulsions (CONEs), compared to the untreated control cultures **(Fig. 3A).**

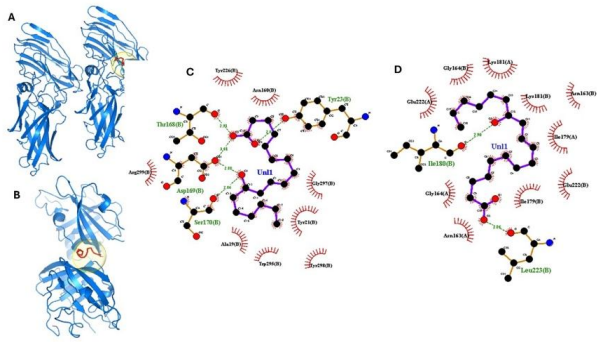

Fig.4 : Structures of Als3 adhesin of *Candida albicans* **(Figure 4A)** and Sortase A of *Streptococcus mutans* **(Fig. 4B).** Ricinoleic acid forming multiple hydrogen bonds with Thr168 (B), Asp169 (B), Ser170 (B), and Tyr23 (B) in Als3 adhesin, along with hydrophobic interactions with Arg299 (B), Ala19 (B), Trp295 (B), Tyr298 (B), Tyr21 (B), Gly297 (B), Asn160 (B), and Tyr226 (B) **(Fig. 4C)**.

Binding of Ricinoleic acid to Sortase A via hydrogen bonds with Ile180 (B) and Leu223 (B), and through hydrophobic interactions with Glu222 (A), Gly164 (B), Lys181 (A and B), Asn163 (A and B), Ile179 (A and B), and Glu222 (B) **(Fig.4D).**

Although the PDI value indicates some polydispersity, it remains within an acceptable range for nanoemulsions, ensuring that the droplets were relatively well-dispersed within the system as suggested by Sharma *et al*. (2020). The zeta potential measurement provided insights into the stability of the nanoemulsion. The CONEs

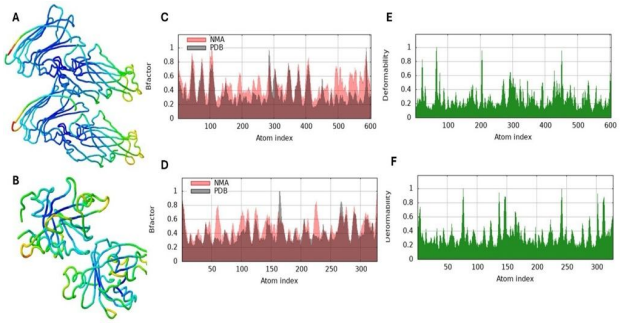

Fig.5: Structural dynamics of the Ricinoleic acid-Als3 adhesin **(Fig.5A)** and Ricinoleic acid-Sortase A complexes **(Fig.5B).**

The B-factor graphs facilitate visualization and comparison between the NMA and the PDB field of the complex, showing the relative mobility of different regions **(Fig. 5C & 5D)**.

The deformability graphs illustrate peaks corresponding to regions in the protein with high deformability, indicating areas of flexibility within the complex **(Fig. 5E & 5F).**

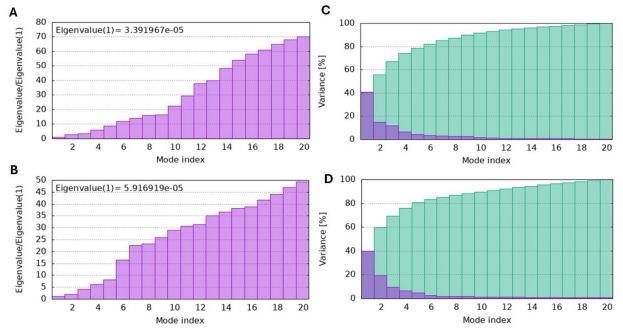

Fig.6: The eigenvalue for the ricinoleic acid-Als3 adhesin complex showing high deformity, indicating a less rigid structure **(Fig. 6A).**

The eigenvalue for the ricinoleic acid-Sortase A complex indicating considerable deformability **(Fig. 6B)**.

The variance graphs show individual variance by red bars and cumulative variance by green bars, with a high degree of cumulative variance indicating overall flexibility of the complexes **(Fig. 6C & 6D)**.

exhibited a negative zeta potential value of -24.69 ± 1.8 mV. Zeta potential values more negative than -30 mV or more positive than +30 mV are generally considered indicative of good colloidal stability due to significant electrostatic repulsion between droplets, which inhibits flocculation and coalescence. Although the zeta potential of CONEs was slightly less negative than -30 mV, it still suggests a reasonably stable nanoemulsion system.

The surfactant used in the preparation of CONEs, Tween 80, played a crucial role in stabilizing the nanoemulsion. Due to its hydrophilic-lipophilic balance (HLB = 15), Tween 80 effectively reduced

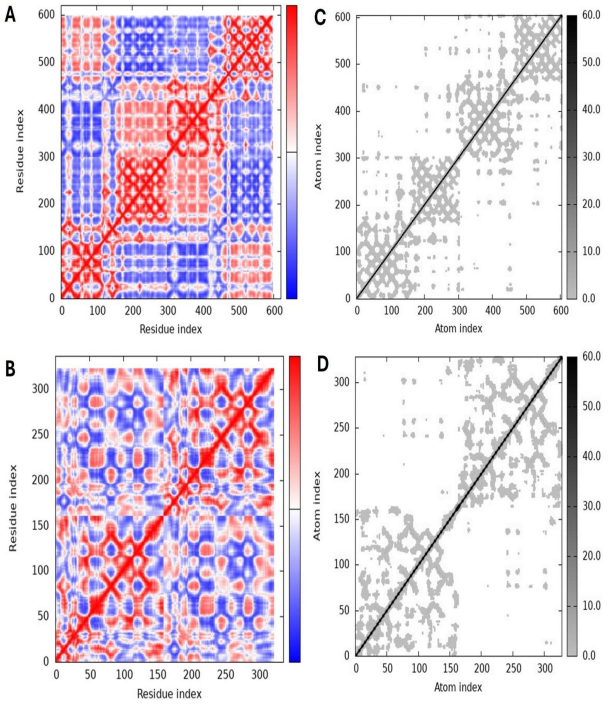

Fig.7: The co-variance maps display the correlated motions between residue pairs **(Fig.7A & 7B),** red indicating correlated motion, white indicating uncorrelated motion, and blue indicating anti-correlated motion.

The elastic network map showing the connections between atoms **(Fig.7C & 7D)**, the darker grey regions represent stiffer areas of the complex.

the interfacial tension between the castor oil and water phases, facilitating the formation of smaller droplets. Additionally, Tween 80, being a small-molecule surfactant, has a higher efficiency in adsorbing onto the droplet surfaces compared to polymer-based surfactants, further enhanced by the ultrasonication process. This rapid absorption decreases the droplet size and prevents recoalescence, contributing to the stability of the nanoemulsion.

Minimum Inhibitory Concentration (MIC) Assay

The minimum inhibitory concentration (MIC) assay was performed to evaluate the antibacterial and antifungal activities of Castor oil nanoemulsion (CONEs) against *Streptococcus mutans*, *Candida albicans*, and their mixed cultures. The MIC values were determined by treating the microorganisms with various concentrations of CONEs (10, 25, 50, 75, and

100 µg/ml) and measuring optical density at 600 nm (Guidotti-Takeuchi *et al*. 2022).

The results indicated that the MIC of CONEs for *Streptococcus mutans* was 50 µg/ml, demonstrating substantial antibacterial effects. For *Candida albicans*, the MIC was higher, at 75 µg/ml, indicating a relatively higher resistance of this fungus to the nanoemulsion treatment compared to *S. mutans*. In the mixed culture condition, where both microorganisms were present, the MIC value increased to 100 µg/ml. This suggests that the presence of both organisms together in a mixed culture increases the overall resistance to the nanoemulsion treatment (Rivera-Quiroga et al., 2020).

These findings highlight the potent antimicrobial activity of CONEs, with significant inhibitory effects on both *S. mutans* and *C. albicans*. The higher MIC value observed in mixed cultures could be attributed to the synergistic protection mechanisms employed by the biofilm matrix, which is known to enhance microbial resistance to antimicrobial agents.

Our results are consistent with prior studies demonstrating the efficacy of nanoemulsions in inhibiting microbial growth. For instance, previous research has shown that essential oils, when formulated into nanoemulsions, exhibit lower MIC values and enhanced antibacterial properties compared to their bulk counterparts. The enhanced antibacterial activity of CONEs can be attributed to the reduced droplet size and increased surface area, which facilitate better interaction with microbial cells.

Disc Diffusion Assay

To further evaluate the antimicrobial efficacy of Castor oil nanoemulsion (CONEs) against *Streptococcus mutans*, *Candida albicans*, and their mixed cultures, a disc diffusion assay was conducted (Haq *et al*. 2023). The assay measured the diameter of the inhibition zones (ZOI) around discs loaded with CONEs at the minimum inhibitory concentration (MIC) and half MIC.

The results demonstrated clear zones of inhibition, indicating the antimicrobial action of CONEs. The diameter of the inhibition zone for *Streptococcus mutans* was found to be 22±1.8 mm, while for *Candida albicans* it was 19±2.2 mm. The mixed culture condition exhibited a larger inhibition zone of 11±1.3 mm. The appearance of these zones around the CONEs-loaded discs confirmed the significant antimicrobial activity against both bacteria and fungi *(Higa et al*. 2022). These findings are consistent with previous reports that nanoemulsions enhance the delivery and efficacy of antimicrobial agents due to their smaller droplet size and increased surface area, which facilitate better interaction with microbial cell membranes. The larger zone of inhibition observed in the mixed culture could be attributed to the synergistic effect of CONEs on the combined biofilm matrix, which is known to enhance microbial resistance when treated individually.

In comparison to other studies, our results show a stronger antimicrobial effect of CONEs. For instance, earlier research using essential oil-based nanoemulsions reported inhibition zones for various pathogens in the range of 11-14 mm. The larger inhibition zones observed in our study suggest that CONEs might have a more potent antimicrobial action, possibly due to the effective formulation and stabilization provided by the nanoemulsion process.

Biofilm Biomass Reduction

To determine the impact of Castor oil nanoemulsions (CONEs) on the biofilm biomass of *Streptococcus mutans* and *Candida albicans*, both individual and mixed cultures were allowed to form biofilms in the presence of CONEs at half of the MIC and MIC concentrations. After 48 hours of incubation, the biofilm biomass was evaluated using crystal violet staining.

The crystal violet assay results indicated a significant reduction in biofilm biomass upon treatment with CONEs. Specifically, the biofilm biomass of *Streptococcus mutans* was reduced by 73%, *Candida albicans* by 61%, and the mixed culture by 48%, as compared to the untreated control by MIC of CONEs (Fig. 2A). This reduction

demonstrates the potent antibiofilm activity of CONEs against these periodontal pathogens (Srivastava *et al*. 2020).

The reduction in biofilm biomass can be attributed to two primary mechanisms. First, the CONEs likely reduce the number of sessile cells within the biofilm, effectively decreasing the overall cell density (Cattò and Cappitelli, 2019). Second, the nanoemulsion may inhibit the production of extracellular polymeric substances (EPS), which serve as the binding matrix for biofilm formation and maintenance. By disrupting EPS production, CONEs weaken the structural integrity of the biofilm, making it more susceptible to removal and antimicrobial treatment (Samrot *et al*. 2021).

These findings align with previous studies that have shown the efficacy of nanoemulsions in disrupting biofilms (Li *et al*. 2021). The ability of CONEs to significantly reduce biofilm biomass highlights their potential as an effective treatment strategy for periodontitis. The reduction of biofilm biomass not only helps in managing the existing infection but also prevents the recurrence and persistence of biofilm-associated pathogens.

Reduction in Sessile Cell Counts

After treating biofilms with the MIC of Castor oil nanoemulsions (CONEs) and incubating for 48 hours, we assessed the number of sessile cells using the spread plate technique. The results showed a substantial reduction in the number of sessile cells within the biofilms of both individual and mixed cultures (Guidotti-Takeuchi *et al*. 2022). The MIC of CONEs resulted in a reduction of sessile cells by 2.7 log (CFU/ml) for *Streptococcus mutans*, 2.3 log (CFU/ml) for *Candida albicans*, and 1.9 log (CFU/ml) for the mixed culture (Fig. 2B). This significant decrease in sessile cell numbers indicates the effectiveness of CONEs in disrupting the biofilm and reducing the viability of biofilm-associated cells (Barbosa *et al*. 2016).The sessile cell counting study corroborates the findings from the biofilm biomass reduction assay, suggesting that one of the primary mechanisms by which CONEs reduce biofilm biomass is by decreasing the number of viable sessile cells. By effectively reducing the population of sessile cells, CONEs help in weakening the biofilm structure and making it more susceptible to antimicrobial treatment and mechanical removal (Cattò and Cappitelli, 2019). These findings are consistent with previous research that highlights the efficacy of nanoemulsions in targeting biofilm-associated cells. The ability of CONEs to significantly reduce sessile cell counts underscores their potential as a therapeutic agent for managing periodontitis, as it helps in controlling the persistent and resistant nature of biofilm-associated infections.

Reduction in EPS Production

Another contributing factor to the reduction in biofilm biomass is the decreased production of extracellular polymeric substances (EPS). EPS acts as a binding matrix, embedding sessile cells within the biofilm and providing structural integrity and protection to the microbial community (More *et al*. 2014).

Our results demonstrated that treatment with the MIC of Castor oil nanoemulsions (CONEs) significantly reduced EPS production in the biofilms formed by *Streptococcus mutans* and *Candida albicans*. Specifically, the EPS production was reduced by 2.3 times for S. mutans, 2.1 times for *C. albicans*, and 1.65 times for the mixed culture, compared to the untreated control (Lemoine *et a*l. 2020) (Fig. 3C).

The observed reduction in EPS production is crucial for the disruption of biofilms (Fig. 3A), as the EPS matrix is integral to the biofilm's stability and resistance to antimicrobial agents. By diminishing the EPS production, CONEs effectively weaken the biofilm structure, making the embedded sessile cells more vulnerable to antimicrobial treatments and mechanical disruption.These findings align with previous studies that have highlighted the importance of targeting EPS production as a strategy for biofilm control. The significant decrease in EPS production further supports the potential of CONEs in managing biofilm-associated infections, particularly in the context of periodontal disease, where robust biofilm formation is a key challenge.

In silico study

The in silico docking study revealed that ricinoleic acid exhibits strong binding affinities with both Als3 adhesin of *Candida albicans* (Fig.4A) and Sortase A of *Streptococcus mutans* (Fig. 4B), with binding energies of -5.8 kcal/mol and -5.7 kcal/mol, respectively. These values suggest a high binding affinity, indicating the potential of ricinoleic acid as an effective inhibitor for these proteins, which are critical for biofilm formation and pathogenicity. Detailed interaction analysis showed that ricinoleic acid forms multiple hydrogen bonds with Thr168 (B), Asp169 (B), Ser170 (B), and Tyr23 (B) in Als3 adhesin, along with hydrophobic interactions with residues such as Arg299 (B), Ala19 (B), Trp295 (B), Tyr298 (B), Tyr21 (B), Gly297 (B), Asn160 (B), and Tyr226 (B) (Figure 4C). This robust interaction profile suggests that ricinoleic acid can significantly hinder the function of Als3 adhesin, thereby reducing the adhesion and biofilm formation capability of *Candida albicans*. Similarly, ricinoleic acid binds to Sortase A via hydrogen bonds with Ile180 (B) and Leu223 (B), and through hydrophobic interactions with Glu222 (A), Gly164 (B), Lys181 (A and B), Asn163 (A and B), Ile179 (A and B), and Glu222 (B) (Fig. 4D). These extensive interactions imply a strong binding to Sortase A, potentially inhibiting its role in biofilm formation and pathogenicity of *Streptococcus mutans*. Comparative analysis with other known inhibitors demonstrates that the binding affinities of ricinoleic acid are significantly high, positioning it as a potent inhibitor. Visualization of these interactions using PyMOL and LigPlot confirmed the binding sites and detailed interactions, highlighting how ricinoleic acid can effectively inhibit these proteins. The comprehensive interaction profile, including multiple hydrogen bonds and hydrophobic contacts, suggests that ricinoleic acid could disrupt the biofilm formation and maintenance mechanisms, reducing the virulence and persistence of these pathogens. These findings underline the therapeutic potential of ricinoleic acid, warranting further experimental validation to explore its efficacy in treating biofilm-associated infections (Martorano-Fernandes *et al*. 2023).

The molecular dynamics simulation study provided valuable insights into the structural dynamics of the ricinoleic acid-Als3 adhesin (Fig. 5A) and ricinoleic acid-Sortase A complexes (Fig.5B). The normal mode analysis (NMA) results for the ricinoleic acid-Als3 adhesin complex are depicted in Figure 5C. The deformability graph (Fig. 5E & 5F) illustrates peaks corresponding to regions in the protein with high deformability, indicating areas of flexibility within the complex. The B-factor graph (Fig.5C & 5D) facilitates easy visualization and comparison between the NMA and the PDB field of the complex, showing the relative mobility of different regions.

The eigenvalue for the ricinoleic acid-Als3 adhesin complex was found to be 3.391967e-05 (Fig. 6A). This low eigenvalue signifies that the complex is highly deformable, indicating a less rigid structure that can adapt to conformational changes more easily. Similarly, the ricinoleic acid-Sortase A complex exhibited an eigenvalue of 5.916919e-05, also indicative of considerable deformability (Fig.6B). The variance graph (Fig.6C & 6D) shows individual variance by red bars and cumulative variance by green bars, with a high degree of cumulative variance indicating overall flexibility of the complexes.

The co-variance map (Fig.7A & 7B) displays the correlated motions between residue pairs, with red indicating correlated motion, white indicating uncorrelated motion, and blue indicating anti-correlated motion. The elastic network map (Fig.7C & 7D) highlights the connections between atoms, where darker gray regions represent stiffer areas of the complex.

These results suggest that both ricinoleic acid-Als3 adhesin and ricinoleic acid-Sortase A complexes possess significant flexibility and low rigidity, as indicated by their low eigenvalues. This flexibility might enhance their binding interactions and stability, making ricinoleic acid an effective inhibitor against these targets. The observed high deformability and satisfactory results from the variance, co-variance, and elastic network maps further support the potential of ricinoleic acid as a promising candidate for disrupting biofilm formation and reducing the virulence of *Candida albicans* and *Streptococcus mutans*. These findings highlight the importance of considering molecular dynamics in the development of novel antimicrobial agents.

CONCLUSION

The comprehensive characterization and antimicrobial efficacy evaluation of CONEs highlight their potential as effective agents against biofilm-associated infections. The nano-sized droplets, facilitated by ultrasonic emulsification, along with the stabilizing effect of Tween 80, ensure the stability and uniformity of the nanoemulsion. The significant reductions in biofilm biomass, sessile cell counts, and EPS production, along with strong binding affinities observed in in silico studies, underscore the therapeutic potential of CONEs, particularly in the context of periodontal disease.

DECLARATION

Conflict of Interest. Authors declare no conflict of interest.

REFERENCES

Bachtiar, E.W., Bachtiar, B.M. 2018. Relationship between Candida albicans and Streptococcus mutans in early childhood caries, evaluated by quantitative PCR. *F1000 Res*. **7**:1645. https://doi.org/10.12688/f1000research.16275.2

Barbosa, J.O., Rossoni, R.D., Vilela, S.F.G., De Alvarenga, J.A., Velloso, M.D.S., Prata, M.C.D.A., Jorge, A.O.C., Junqueira, J.C. 2016. *Streptococcus mutans* Can Modulate Biofilm Formation and Attenuate the Virulence of *Candida albicans*. *PLoS ONE* **11**: e0150457. https://doi.org/10.1371/journal.pone.0150457

Cattò, C., Cappitelli, F.,2019. Testing Anti-Biofilm Polymeric Surfaces: Where to Start? *Inter. J.Mol.Sci.* **20**: 3794. https://doi.org/10.3390/ijms20153794

Das, S.K., Vishakha, K., Das, S., Ganguli, A. 2023. Antibacterial and antibiofilm activities of nanoemulsion coating prepared by using caraway oil and chitosan prolongs the shelf life and quality of bananas. *Appl. Food Res*. **3**: 100300. https://doi.org/10.1016/j.afres.2023.100300

El-Naby, S.S.I.A., Abdou, M.Sh., Metayi, M.H.A., Mahmoud, F.H.E., El-Habal, N.A.M., Abdel-Megeed, A., Cipriano-Salazar, M. 2024. Development and evaluation of castor oil nanoemulsion on the cotton leaf worm Spodoptera littoralis (Boisd.) and its adverse effects on the reproductive system of albino rats. *Biomass Conv. Bioref.* **14**: 2629–2641. https://doi.org/10.1007/s13399-021-02245-8

Espinel-Ingroff, A., Kerkering, T.M., Goldson, P.R., Shadomy, S. 1991. Comparison study of broth macrodilution and microdilution antifungal susceptibility tests. *J. Clin. Microbiol*. **29**: 1089–1094. https://doi.org/10.1128/jcm.29.6.1089-1094.1991

Forssten, S.D., Björklund, M., Ouwehand, A.C. 2010. Streptococcus mutans, Caries and Simulation Models. *Nutrients* **2**: 290–298. https://doi.org/10.3390/nu2030290

Guidotti-Takeuchi, M., De Morais Ribeiro, L.N.D.M., Dos Santos, F.A.L., Rossi, D.A., Lucia, F.D., De Melo, R.T. 2022. Essential Oil-Based Nanoparticles as Antimicrobial Agents in the Food Industry. *Microorganisms* **10**: 1504. https://doi.org/10.3390/microorganisms10081504

Haq, N., Shahid, M., Alaofi, A.L., Ahmad, Z.H., Alrayyes, Y.F., Alsarra, I.A., Shakeel, F. 2023. Evaluation of the Physicochemical and Antimicrobial Properties of Nanoemulsion-Based Polyherbal Mouthwash. *ACS Omega* **8**: 41755–41764. https://doi.org/10.1021/acsomega.3c06176

Higa, B., Cintra, B.S., Álvarez, C.M., Ribeiro, A.B., Ferreira, J.C., Tavares, D.C., Enriquez, V., Martinez, L.R., Pires, R.H. 2022. Ozonated oil is effective at killing *Candida* species and Streptococcus mutans biofilm-derived cells under aerobic and microaerobic conditions. *Medical Mycol.* **60:** myac055. https://doi.org/10.1093/mmy/myac055

Hobson, C., Chan, A.N., Wright, G.D. 2021. The Antibiotic Resistome: A Guide for the Discovery of Natural Products as Antimicrobial Agents. *Chem. Rev*. **121**: 3464–3494. https://doi.org/10.1021/acs.chemrev.0c01214

Katzer, T., Chaves, P., Bernardi, A., Pohlmann, A.R., Guterres, S.S., Beck, R.C.R. 2014. Castor oil and mineral oil nanoemulsion: development and compatibility with a soft contact lens. *Pharmaceut. Devel. Technol*. **19**: 232–237. https://doi.org/10.3109/10837450.2013.769569

Kavanagh, A., Ramu, S., Gong, Y., Cooper, M.A., Blaskovich, M.A.T. 2019. Effects of Microplate Type and Broth Additives on Microdilution MIC Susceptibility Assays. *Antimicrob. Agents Chemother*. **63**: e01760-18. https://doi.org/10.1128/AAC.01760-18

Könönen, E., Gursoy, M., Gursoy, U. 2019. Periodontitis: A Multifaceted Disease of Tooth-Supporting Tissues. *J.Clin.Med.* **8**: 1135. https://doi.org/10.3390/jcm8081135

Lemoine, V., Bernard, C., Leman-Loubière, C., Clément-Larosière, B., Girardot, M., Boudesocque-Delaye, L., Munnier, E., Imbert, C. 2020. Nanovectorized Microalgal Extracts to Fight Candida albicans and Cutibacterium acnes Biofilms: Impact of Dual-Species Conditions. *Antibiotics* **9**: 279. https://doi.org/10.3390/antibiotics9060279

Li, C.-H., Landis, R.F., Makabenta, J.M., Nabawy, A., Tronchet, T., Archambault, D., Liu, Y., Huang, R., Golan, M., Cui, W., Mager, J., Gupta, A., Schmidt-Malan, S., Patel, R., Rotello, V.M. 2021. Nanotherapeutics using all-natural materials. Effective treatment of wound biofilm infections using crosslinked nanoemulsions. *Mater. Horiz*. **8**: 1776–1782. https://doi.org/10.1039/D0MH01826K

Loureiro Contente, D.M., Pereira, R.R., Rodrigues, A.M.C., Da Silva, E.O., Ribeiro-Costa, R.M., Carrera Silva-Júnior, J.O., 2020. Nanoemulsions of Acai Oil: Physicochemical Characterization for the Topical Delivery of Antifungal Drugs. *Chem. Eng.Amp. Technol.* 43: 1424–1432. https://doi.org/10.1002/ceat.201900627

Martínez-García, M., Hernández-Lemus, E., 2021. Periodontal Inflammation and Systemic Diseases: An Overview. *Front. Physiol*. **12**: 709438. https://doi.org/10.3389/fphys.2021.709438

Martorano-Fernandes, L., Goodwine, J., Ricomini-Filho, A., Nobile, C., Del Bel Cury, A. 2023. *Candida albicans* Adhesins Als1 and Hwp1 Modulate Interactions with *Streptococcus mutans*. *Microorganisms* 11: 1391. https://doi.org/10.3390/microorganisms11061391

Mendhe, S., Badge, A., Ugemuge, S., Chandi, D. 2023. Impact of Biofilms on Chronic Infections and Medical Challenges. *Cureus*. **15:** e48204 https://doi.org/10.7759/cureus.48204

Mittal, R.P., Jaitak, V. 2019. Plant-Derived Natural Alkaloids as New Antimicrobial and Adjuvant Agents in Existing Antimicrobial Therapy. *CDT* **20**: 1409–1433. https://doi.org/10.2174/1389450120666190618124224

Morales, D.K., Hogan, D.A. 2010. *Candida albicans* Interactions with Bacteria in the Context of Human Health and Disease. *PLoS Pathog*. **6**: e1000886. https://doi.org/10.1371/journal.ppat.1000886

More, T.T., Yadav, J.S.S., Yan, S., Tyagi, R.D., Surampalli, R.Y. 2014. Extracellular polymeric substances of bacteria and their potential environmental applications. *J. Environmen. Managt.* **144**: 1–25. https://doi.org/10.1016/j.jenvman.2014.05.010

Okonogi, S., Phumat, P., Khongkhunthian, S., Chaijareenont, P., Rades, T., Müllertz, A. 2021. Development of Self-Nanoemulsifying Drug Delivery Systems Containing 4-Allylpyrocatechol for Treatment of Oral Infections Caused by *Candida albicans*. *Pharmaceutics* **13**: 167. https://doi.org/10.3390/pharmaceutics13020167

Oliveira, A.E.M.F.M., Duarte, J.L., Cruz, R.A.S., Conceição, E.C.D., Carvalho, J.C.T., Fernandes, C.P. 2017. Utilization of dynamic light scattering to evaluate Pterodon emarginatus oleoresin-based nanoemulsion formation by non-heating and solvent-free method. *Revista Brasileira de Farmacognosia* **27**: 401–406. https://doi.org/10.1016/j.bjp.2016.11.005

Pathania, R., Khan, H., Kaushik, R., Khan, M.A. 2018. Essential Oil Nanoemulsions and their Antimicrobial and Food Applications. *Curr. Res. Nutr. Food Sci.* **6**: 626–643. https://doi.org/10.12944/CRNFSJ.6.3.05

Poorani, G., Uppuluri, S., Uppuluri, K.B., 2016. Formulation, characterization, in vitro and in vivo evaluation of castor oil based self-nano emulsifying levosulpiride delivery systems. *J. Microencapsulation* **33**: 535–543. https://doi.org/10.1080/02652048.2016.1223199

Rajamani, S., Sandy, R., Kota, K., Lundh, L., Gomba, G., Recabo, K., Duplantier, A., Panchal, R.G. 2019. Robust biofilm assay for quantification and high throughput screening applications. *J. Microbiologic. Methods* **159**: 179–185. https://doi.org/10.1016/j.mimet.2019.02.018

Ray, R.R. 2023. Periodontitis: An Oral Disease with Severe Consequences. *Appl. Biochem. Biotechnol.* **195**: 17–32. https://doi.org/10.1007/s12010-022-04127-9

Rivera-Quiroga, R.E., Cardona, N., Padilla, L., Rivera, W., Rocha-Roa, C., Diaz De Rienzo, M.A., Morales, S.M., Martinez, M.C. 2020. *In Silico* Selection and *In Vitro* Evaluation of New Molecules That Inhibit the Adhesion of *Streptococcus mutans* through Antigen I/II. *IJMS* **22**: 377. https://doi.org/10.3390/ijms22010377

Rudrapal, M. (Ed.) 2023. Polyphenols: Food, Nutraceutical, and Nanotherapeutic Applications, 1st ed. Wiley. https://doi.org/10.1002/9781394188864

Samrot, A.V., Abubakar Mohamed, A., Faradjeva, E., Si Jie, L., Hooi Sze, C., Arif, A., Chuan Sean, T., Norbert Michael, E., Yeok Mun, C., Xiao Qi, N., Ling Mok, P., Kumar, S.S. 2021. Mechanisms and Impact of Biofilms and Targeting of Biofilms Using Bioactive Compounds—A Review. *Medicina* **57**: 839. https://doi.org/10.3390/medicina57080839

Sharma, N., Bachalo, W.D., Agarwal, A.K. 2020. Spray droplet size distribution and droplet velocity measurements in a firing optical engine. *Physics of Fluids* **32**: 023304. https://doi.org/10.1063/1.5126498

Singh, S., Singh, S.K., Chowdhury, I., Singh, R. 2017. Understanding the Mechanism of Bacterial Biofilms Resistance to Antimicrobial Agents. *The Open Microbiol. J.* **11**: 53–62. https://doi.org/10.2174/1874285801711010053

Srivastava, N., Ellepola, K., Venkiteswaran, N., Chai, L.Y.A., Ohshima, T., Seneviratne, C.J. 2020. *Lactobacillus plantarum* 108 Inhibits *Streptococcus mutans* and *Candida albicans* Mixed-Species Biofilm Formation. *Antibiotics* **9**: 478. https://doi.org/10.3390/antibiotics9080478

Tullio, V., Nostro, A., Mandras, N., Dugo, P., Banche, G., Cannatelli, M.A., Cuffini, A.M., Alonzo, V., Carlone, N.A. 2007. Antifungal activity of essential oils against filamentous fungi determined by broth microdilution and vapour contact methods. *J .Appl. Microbiol.* **102**: 1544–1550. https://doi.org/10.1111/j.1365-2672.2006.03191.x

Van Vuuren, S., Viljoen, A. 2011. Plant-Based Antimicrobial Studies – Methods and Approaches to Study the Interaction between Natural Products. *Planta Med.* **77**: 1168–1182. https://doi.org/10.1055/s-0030-1250736

Wallock-Richards, D.J., Marles-Wright, J., Clarke, D.J., Maitra, A., Dodds, M., Hanley, B., Campopiano, D.J. 2015. Molecular basis of Streptococcus mutans sortase A inhibition by the flavonoid natural product trans-chalcone. *Chem. Commun*. **51**: 10483–10485. https://doi.org/10.1039/C5CC01816A